JOURNAL OF MAGNETIC RESONANCE **126,** 164–182 (1997)
ARTICLE NO. MN971161

The Signs of Frequencies and Phases in NMR

Malcolm H. Levitt*

Physical Chemistry Division, Stockholm University, S-10691 Sweden

Received September 3, 1996; revised March 11, 1997

The signs of radiofrequency phases and frequencies used in NMR are examined carefully. Some fundamental problems with current usage are exposed by simple examples. The entire chain of events leading to the NMR spectrum is examined closely, including generation and phase-shifting of the radiofrequency carrier wave, nuclear-spin dynamics in the presence of the radiofrequency field, quadrature detection, signal digitization, post-digitization phase shifting, Fourier transformation, and spectral presentation. Recommendations are given for software modifications which should facilitate the correspondence between pulse programming, spectral presentation, and spin dynamical theory. © 1997 Academic Press

INTRODUCTION

This paper addresses the signs of the phases and frequencies used to perform an NMR experiment, understand the spin dynamics, and to present NMR spectra. I come to some rather disturbing conclusions. I argue that current usage introduces sign inconsistencies at almost every stage. The phase angles which are relevant to the spin dynamics are usually opposite in sign to the values appearing in pulse programs. The frequency axis commonly used to label the spectrum is usually opposite in sign to the true precession frequency of the magnetization components in the rotating frame. Similar inconsistencies apply to the receiver reference phase and to the post-digitization phase shift applied at the outputs of the analog–digital converters. These sign errors appear to have passed unnoticed because in many cases they cancel mutually.

In the past, it has usually been possible to gloss over these issues. However, it is becoming increasingly commonplace to perform detailed manipulations of spin systems with a complex mix of spin interactions. For example, solid-state NMR is often performed on systems with small groups of coupled spins, where indirect and through-space magnetic dipolar couplings, shielding anisotropies, and sometimes quadrupolar couplings all coexist. For example, the accurate simulation of spin dynamical phenomena such as rotational resonance (*1–3*) requires careful handling of relative signs. Solution NMR is generally more forgiving, but some areas are also fraught with subtle sign problems, for example, cross-correlated relaxation (*4–9*), nuclear demagnetizing field effects (*10–13*), and phase or frequency shifts induced by sample movement through nonuniform radiofrequency fields (*14–16*).

There are semantic obstacles to the careful treatment of signs in NMR. It is rather striking that scientific English distinguishes between the *speed* and *velocity* of linear motion, whereas no analogous terms exist for the frequency of rotational motion (J. S. Waugh once tried to remedy this defect by introducing the term ''avis'' to signify ''angular velocity, inverse seconds''). This semantic void causes confusion in NMR, because the term (angular) frequency has a double meaning. For example, the radiofrequency synthesizer of a spectrometer oscillates with a certain frequency, by definition positive since it merely reflects the number of electrical oscillations per unit time. By multiplying the number of cycles per second by 2π, one obtains the (angular) carrier frequency $|\omega^{\mathrm{carrier}}|$, a positive number. Note that it would be as meaningless to assign a negative value to the carrier frequency as it would be to assign an object a negative speed. In contrast, true rotational motion does have a meaningful sign. In a right-handed coordinate system, anticlockwise motion looking down the rotation axis is defined as positive, while clockwise motion is defined as negative. For example, the Larmor precession of nuclear spins around the magnetic field has a definite sign (negative for spins of positive magnetogyric ratio γ, and positive for spins of negative magnetogyric ratio γ). The Larmor frequency is a different type of physical quantity to the spectrometer carrier frequency.

To fill the semantic vacuum, this article distinguishes consistently between ''signed'' and ''unsigned'' angular frequencies. The use of a symbol ω indicates a signed angular frequency, expressing a physical rotation about an axis, for example, the Larmor precession frequency of nuclear spins about the field. The modulus $|\omega|$ is used for frequencies which are positive by definition, such as those corresponding to a number of events per second, multiplied by 2π.

To unravel the relevant sign issues, the entire chain of events involved in producing an NMR spectrum is examined closely. This includes the generation of the RF pulses, the excitation of spin coherences, the electromagnetic induction of electrical signals in the receiver coil, quadrature detection,

* E-mail: mhl@physc.su.se.

1090-7807/97 $25.00

the post-digitization phase shifting of the signal, Fourier transformation, and finally, the presentation of the spectrum. Much of this discussion is rather elementary. However, an unusual level of explicitness seems justified. In my view, the general tendency to take most of this reasoning for granted has probably contributed to the persistence of the errors. Even those readers who disagree with the arguments, and conclude that a rationalization of sign usage is unnecessary, may find that a compilation of the reasoning in one place is a useful basis for discussion.

After the detailed examination of the NMR experiment, the need for a consistent treatment of signs is highlighted by simple examples. Concrete suggestions for future practice are then given. These include not only revised labeling and plotting of spectra, but also modifications in the pulse programming and data processing software.

One of the main recommendations of this article is that the *phases* involved in the NMR experiment should be adjusted to account for the sign of the magnetogyric ratio of the resonant spin species. To clarify this issue, two distinct symbols for phases are used in this article. The symbol ψ is used for ''ordinary'' phases, as generated by the spectrometer electronics, or in the case of the post-digitization phase shift, by the signal processing hardware at the outputs of the analog–digital converters (ADCs). These phases take their conventional meaning according to normal usage in electronics and mathematics. For example, the carrier wave of the spectrometer is given by

$$s^{\text{carrier}}(t) \cong \cos(|\omega^{\text{carrier}}|t + \psi^{\text{carrier}}), \qquad [1]$$

where ψ^{carrier} is the radiofrequency carrier phase. On current spectrometers, the pulse program software allows direct control of this phase. It is generally assumed that this radiofrequency phase shift is transferred without change to the rotating-frame nutation axes governing the spin dynamics. As will be shown, this is incorrect in general. In this article, phases of direct importance to the spin dynamics are denoted by the symbol ϕ and are related to the ''raw'' phases ψ through

$$\phi = -(\text{sign } \gamma)\psi, \qquad [2]$$

where sign γ is equal to -1 if γ is negative, and to 1 otherwise. This relationship applies not only to the RF phases at the excitation stage, but also to the receiver reference phase, and the post-digitization processing of the signals at the outputs of the ADCs. This article recommends that the spectrometer software should allow direct control of the ''γ-sensitive'' phases ϕ, rather than the raw phases ψ. The phases used in pulse programs would then correspond directly to the phases used in spin dynamical calculations. At present, this is not the case, as discussed below.

The second main problem discussed in this article is connected with the detection and processing of signals from spins of negative magnetogyric ratio γ. It is argued that current detection schemes actually produce *quadrature image spectra* for such spins. This has passed by without notice probably because this error cancels out the above-mentioned error associated with the sign of the nutation axis phase shifts. However, rationalization of the nutation axis phase shifts also necessitates careful attention to this problem. A corrected data processing scheme for negative γ signals is suggested.

At first sight, it is surprising that any attention need be given to the sign of the Larmor frequency in ordinary NMR experiments. After all, signal detection usually takes place by a single RF coil, which cannot distinguish between magnetization components rotating in opposite senses. This is in fact correct, and neither the software nor the hardware of a single-coil NMR spectrometer needs to be changed in order to observe signals from spins with the opposite sign of γ. However, this article is concerned with a deeper problem—not merely producing NMR signals, but understanding them on a microscopic level. For this purpose, it is important that there is a clear connection between the controllable spectrometer parameters and the spin dynamics, and that proper account is taken of the signs of the interactions between the spins and their molecular surroundings. It is on this point that improvements are needed, in the author's opinion.

Before proceeding, I emphasize that the sense of the nutation axis phase shift (which governs the *direction* of the nutation axis) must not be confused with the sense of the nutation itself. The sense of the nutation has aroused controversy in the NMR world, which appears to be divided into two schools, one of which advocates a ''positive nutation'' convention, and the other a ''negative nutation'' convention. Unlike the sense of the phase shift, the sense of the nutation has no practical consequences at all, so there is complete freedom on this issue. In this article, I define the rotating frame in such a way as to force a constant positive nutation of the spins, which is mathematically convenient. This conforms to the usage of Ernst and co-workers, and many others. However, the main arguments of this article are completely independent of this choice.

SPIN INTERACTIONS

In this section, I review the principal interactions of spins-$\frac{1}{2}$, with special attention given to signs. This discussion is included mainly for the sake of unambiguity.

The Larmor Frequency

The signed Larmor frequency of nuclear spins with magnetogyric ratio γ is given by

$$\omega_0 = -\gamma B_0, \qquad [3]$$

where B_0 is the static magnetic flux density. In the case of positive γ, the Larmor frequency ω_0 is negative.

The negative sign of the Larmor frequency for spins of positive γ indicates that the spin angular momenta precess around the magnetic field in a clockwise direction, as viewed down the magnetic field lines (Fig. 1). This applies both to individual spins and to the density operator of the spin ensemble.

Spin precession may be described quantum-mechanically by the Schrödinger equation. Define a laboratory coordinate system L, with the z axis along the magnetic field direction. The Hamiltonian of an isolated spin in the laboratory coordinate system is

$$H_0^L = \omega_0 I_z. \qquad [4]$$

Suppose the spin is in a laboratory-frame state $|t_a\rangle^L$ at time t_a. The state $|t_b\rangle^L$ at a later time $t_b > t_a$ may be deduced by integrating the Schrödinger equation

$$\frac{d}{dt}\,|t\rangle^L = -iH_0^L\,|t\rangle^L. \qquad [5]$$

This leads to

$$|t_b\rangle^L = U_0(t_b, t_a)|t_a\rangle^L, \qquad [6]$$

with the propagation operator

$$U_0(t_b, t_a) = \exp\{-i\omega_0(t_b - t_a)I_z\}. \qquad [7]$$

Consider, for example, a single spin-$\frac{1}{2}$, prepared at time t_a in a laboratory frame spin state $|t_a\rangle^L$ with sharply defined angular momentum $+\frac{1}{2}$ along the x axis:

$$I_x|t_a\rangle^L = +\tfrac{1}{2}|t_a\rangle^L. \qquad [8]$$

For example, a suitable state is

$$|t_a\rangle^L = \frac{1}{\sqrt{2}}\{|\alpha\rangle + |\beta\rangle\}, \qquad [9]$$

where $|\alpha\rangle = |\tfrac{1}{2}\rangle$, $|\beta\rangle = |-\tfrac{1}{2}\rangle$, and $|m\rangle$ is an eigenstate of I_z, with eigenvalue m:

$$I_z|m\rangle = m|m\rangle. \qquad [10]$$

After a positive time interval $t_b - t_a = |\pi/(2\omega_0)|$, the spin will have evolved into the state

$$|t_b\rangle^L = \tfrac{1}{2}(1 + i\,\text{sign}\,\gamma)|\alpha\rangle + \tfrac{1}{2}(1 - i\,\text{sign}\,\gamma)|\beta\rangle, \qquad [11]$$

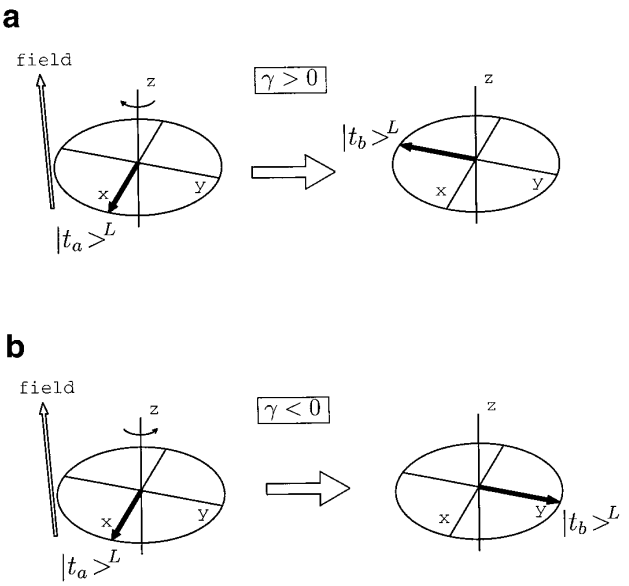

FIG. 1. The sense of spin precession. (a) Case of positive γ. A single spin-$\frac{1}{2}$, prepared in a laboratory-frame quantum state $|t_a\rangle^L$, evolves into a state $|t_b\rangle^L$ over an interval $\tau = \frac{1}{4}|2\pi/\omega_0|$. If the state $|t_a\rangle^L$ is an eigenstate of I_x with eigenvalue $+\frac{1}{2}$, then the state $|t_b\rangle^L$ is an eigenstate of the operator I_y with eigenvalue $-\frac{1}{2}$. This corresponds to spin precession in the negative (clockwise) direction. (b) Case of negative γ. The final state $|t_b\rangle^L$ is an eigenstate of the operator I_y with eigenvalue $+\frac{1}{2}$. This corresponds to spin precession in the positive (anticlockwise) direction.

which has defined angular momentum $-\frac{1}{2}$ sign γ around the y axis:

$$I_y|t_b\rangle^L = -\tfrac{1}{2}(\text{sign}\,\gamma)|t_b\rangle^L. \qquad [12]$$

Spins of positive γ precess in the negative (clockwise) direction around the z axis; spins of negative γ precess in the positive (anticlockwise) direction (Fig. 1).

The behavior of individual spins is also reflected in the behavior of the density operator $\rho^L(t)$ of the spin ensemble

$$\rho^L(t) = \overline{|t\rangle^L\langle t|^L}, \qquad [13]$$

where the bar denotes an ensemble average. For example, an initial spin-density operator proportional to the operator I_x evolves into an operator proportional to $-(\text{sign}\,\gamma)I_y$ over the positive time interval $t_b - t_a = |\pi/(2\omega_0)|$:

$$U_0(t_b, t_a)I_xU_0(t_b, t_a)\dagger = -(\text{sign}\,\gamma)I_y. \qquad [14]$$

The negative sign of ω_0 for spins of positive magnetogyric ratio is a source of much trouble and confusion, as will be seen. Nevertheless, it is a physical fact which cannot be defined away without a greatly contrived and specialized convention, which only shifts the trouble elsewhere. One

might, for example, employ a left-handed coordinate system, or define the z axis of the laboratory reference system to be opposite to the magnetic field direction. Such awkward possibilities are not considered further here.

Chemical Shifts

There are two main conventions for the chemical shifts induced by the electron clouds surrounding the nucleus: In the *shielding* system, the Larmor frequency of a molecular site j is written

$$\omega_0^j = \omega_0^{\text{ref}}(1 - \sigma^j), \qquad [15]$$

which expresses the physical idea that the local flux density at site j is reduced compared to that of an unshielded nucleus by a fraction σ^j. Here ω_0^{ref} is the Larmor frequency of an agreed reference compound exposed to the same macroscopic magnetic flux density (defining $\sigma^{\text{ref}} = 0$). The shielding scale for chemical shifts is particularly widespread in solid-state NMR.

Since ω_0 is *negative* for spins of positive γ, the Larmor frequency shift $-\omega_0^{\text{ref}}\sigma^j$ is *positive* for positive shielding. Electronic shielding causes the Larmor frequency to be less negative, i.e., the Larmor frequency is shifted in the positive direction. For spins of negative γ, on the other hand, the shielding shifts are *negative.*

Liquid-state NMR spectroscopists generally prefer a *deshielding* scale for chemical shifts. In this system, the shielded Larmor frequencies are written

$$\omega_0^j = \omega_0^{\text{ref}}(1 + \delta^j). \qquad [16]$$

For ^{13}C and ^{1}H spectroscopy, ω_0^{ref} usually refers to the reference compound tetramethylsilane (TMS). The Larmor frequency shifts are negative with increasing deshielding δ, for nuclei of positive γ.

The laboratory-frame Zeeman Hamiltonian for spins in site j may therefore be written as either

$$H_j^L = \omega_0(1 - \sigma^j)I_{jz}, \qquad [17]$$

or

$$H_j^L = \omega_0(1 + \delta^j)I_{jz}, \qquad [18]$$

where ω_0^{ref} is here written as ω_0 for simplicity.

The reader is warned that the above usage is not universal and that some workers employ the notation σ for *deshielding.*

Spin–Spin Couplings

The spin Hamiltonian for scalar coupling between spins in sites j and k is universally written as

$$H_{jk}^{\text{scalar}} = 2\pi J_{jk}\mathbf{I}_j \cdot \mathbf{I}_k. \qquad [19]$$

This indicates that if the J coupling is positive, the energy of the spin system is increased when the spin angular momenta are parallel, and is decreased when the spin angular momenta are opposite. The factor 2π is necessary because the J coupling is always given in hertz, while the spin Hamiltonian requires radians per second. Note that the signs of γ of the involved spins are absorbed into the sign of J_{jk} itself: For example, ^{13}C–^{14}N and ^{13}C–^{15}N J couplings are opposite in sign for spins in equivalent molecular sites.

The high-field through-space magnetic dipolar coupling between spins in sites j and k is given by

$$H_{jk}^{\text{direct}} = \langle b_{jk}\tfrac{1}{2}(3\cos^2\theta_{jk} - 1)\rangle,(3I_{jz}I_{kz} - \mathbf{I}_j \cdot \mathbf{I}_k) \qquad [20]$$

where θ_{jk} is the angle between the spin–spin vector and the static magnetic field, and the dipole–dipole coupling constant is

$$b_{jk} = -\left(\frac{\mu_0}{4\pi}\right)\frac{\gamma_j\gamma_k\hbar}{r_{jk}^3}, \qquad [21]$$

in units of radians per second. The angular brackets $\langle\cdots\rangle$ denote an average over rapid molecular motions. The negative sign of b_{jk} indicates that the dipole–dipole coupling decreases the energy of the spin system if the vector joining the spins, and the spin polarizations, are all parallel to the external magnetic field, and the spins have the same sign of γ.

Equations [19] and [21] may be truncated further in the usual way for heteronuclear spin systems in high field.

The Radiofrequency Field

During a radiofrequency pulse p, the spectrometer synthesizer generates an electronic carrier signal of frequency $|\omega^{\text{carrier}}|$ and phase ψ_p:

$$s^{\text{carrier}}(t) = \cos(|\omega^{\text{carrier}}|t + \psi_p). \qquad [22]$$

The carrier frequency $|\omega^{\text{carrier}}/2\pi|$ is simply the number of cycles per second of an oscillating electronic voltage and is by definition positive. The phase shift ψ_p is defined according to standard practice in electronics: The waveform corresponding to $\psi_p = \pi/2$ is ''behind'' the waveform corresponding to $\psi_p = 0$ by a quarter wave (Fig. 2).

The carrier frequency is close to the absolute value of the Larmor frequency, $|\omega^{\text{carrier}}| \cong |\omega_0|$. Usually this carrier wave is generated by a radiofrequency mixing scheme involving combinations of other radiofrequency signals. In this case, care must be taken that the sense of the final phase shift ψ_p of the carrier wave is compatible with Eq. [22] (*17*).

Throughout this article, the origin of the time coordinate

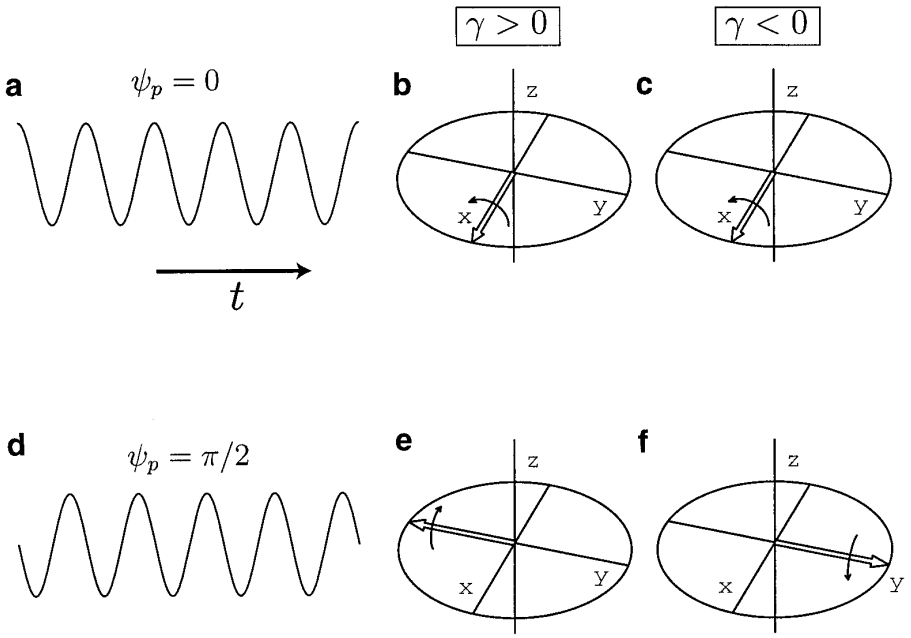

FIG. 2. Correspondence between radiofrequency carrier waves and rotating-frame fields, ignoring resonance offset effects. (a) A radiofrequency wave of frequency $|\omega^{\text{carrier}}|$ and phase $\psi_p = 0$ corresponds to nutation around the x axis for spins of both positive magnetogyric ratio (b) and negative magnetogyric ratio (c). (d) A radiofrequency wave of frequency ω^{carrier} and phase $\psi_p = \pi/2$ corresponds to nutation around the $-y$ axis for spins of positive magnetogyric ratio (e) but around the y axis for spins with negative magnetogyric ratio (f).

$t = 0$ is chosen to coincide with the start of signal acquisition. The time origin is assumed to be reset on each independent RF pulse sequence/signal acquisition scheme. This choice of the time origin is consistent with the definition of Fourier transformation (see below). A consistent choice of time origin is particularly important for rotating samples [see, for example, Ref. (*18*)].

It should be mentioned that current spectrometers do not usually synchronize the pulse sequence gate events with the oscillations of the carrier wave. This implies that the phase origin of the carrier varies randomly from transient to transient. This is undesirable in general, but the effects are generally thought to be minor, except for very short intense RF pulses (*19*). This random overall phase shift is ignored in this article.

We now examine the interaction of the nuclear spins with the RF field. Consider an ensemble of single spins-$\frac{1}{2}$, in sites j with shielding constant σ^j and Larmor frequency ω_0^j, exposed to a RF field of frequency $|\omega^{\text{carrier}}|$ along the x axis of the laboratory reference system L. For simplicity, it is assumed that the RF magnetic flux density at the spins is proportional to the amplified RF carrier wave. We may neglect the constant instrumental phase shift from the propagation delays in the cables and the tuned circuits in the transmission circuitry and the probe. The magnetic flux density experienced by each spin is given by

$$\mathbf{B}(t) = B_0(1 - \sigma^j)\mathbf{e}_z + 2B_{\text{RF}}\cos(|\omega^{\text{carrier}}|t + \psi_p)\mathbf{e}_x, \quad [23]$$

where $\mathbf{e}_x$ and $\mathbf{e}_z$ are unit vectors, and the peak amplitude of the RF flux density at the spins is written $2B_{\text{RF}}$. The spin Hamiltonian in the laboratory frame is

$$H^L(t) = \omega_0^j I_{jz} + 2\omega_{\text{nut}}\cos(|\omega^{\text{carrier}}|t + \psi_p)I_{jx}, \quad [24]$$

defining the (signed) nutation frequency

$$\omega_{\text{nut}} = -\gamma B_{\text{RF}}. \quad [25]$$

The transformation of the spin Hamiltonian to the rotating frame is elementary, but is given in full so as to make clear the propagation of signs. The laboratory frame Hamiltonian is conveniently written as

$$H^L(t) = \omega_0^j I_{jz} + H_+^L(t) + H_-^L(t), \quad [26]$$

where the interaction of the spins with the RF field is decomposed into two components, rotating in opposite senses:

$$H_\pm^L(t) = \tfrac{1}{2}I_j^- \omega_{\text{nut}}\exp\{\pm i(|\omega^{\text{carrier}}|t + \psi_p)\} + \tfrac{1}{2}I_j^+ \omega_{\text{nut}}\exp\{\mp i(|\omega^{\text{carrier}}|t + \psi_p)\}. \quad [27]$$

The H_+^L component represents the interaction of the spins with a field component rotating in the positive sense about the static magnetic field. The H_-^L component represents the

interaction of the spins with a field component rotating in the negative sense.

To analyze the spin dynamics, the spin Hamiltonian is set into a more amenable form by a rotating-frame transformation. The transformed Hamiltonian is given by

$$H(t) = V(t)^{\dagger}H^{L}(t)V(t) - \omega_{\text{frame}}tI_{jz}, \qquad [28]$$

where the frame transformation operator V is given by

$$V(t) = \exp\{-i(\omega_{\text{frame}}t + \phi_{\text{frame}})I_{jz}\}. \qquad [29]$$

The (signed) rotating-frame frequency is denoted ω_{frame}. The initial phase of the rotating frame is denoted ϕ_{frame} and may be chosen arbitrarily.

Proper application of perturbation theory requires that the transformed Hamiltonian is (i) periodic, i.e., $H(t) = H(t + NT)$ where T is the period and N is an arbitrary integer, and (ii) small compared to its own period, i.e., $\|HT\| \ll 1$ where $\|\cdots\|$ indicates the largest difference in eigenvalues (*20*). Both conditions are accomplished in the high-field case ($B_0 \gg B_{\text{RF}}$) if a rotating-frame frequency ω_{frame} is chosen which (i) has the same *magnitude* as that of the carrier wave $|\omega^{\text{carrier}}|$, and (ii) has the same *sign* as the Larmor frequency ω_0. With this choice, the transformed Hamiltonian is periodic with period $T = |2\pi/\omega^{\text{carrier}}|$ and small compared to its own period. The appropriate choice of the rotating-frame frequency is therefore

$$\omega_{\text{frame}} = -(\text{sign } \gamma)|\omega^{\text{carrier}}|, \qquad [30]$$

in which case the rotating-frame Hamiltonian is

$$H(t) = (\omega_0^j - \omega_{\text{frame}})I_{jz} + H_{+}(t) + H_{-}(t), \qquad [31]$$

with the components

$$H_{\pm}(t) = \tfrac{1}{2}I_j^{-}\omega_{\text{nut}} \times \exp\{i[(\pm|\omega^{\text{carrier}}| - \omega_{\text{frame}})t \pm \psi_p - \phi_{\text{frame}}]\} + \tfrac{1}{2}I_j^{+}\omega_{\text{nut}}\exp\{-i[(\pm|\omega^{\text{carrier}}| - \omega_{\text{frame}})t \pm \psi_p - \phi_{\text{frame}}]\}. \qquad [32]$$

In the case of *positive* γ, the H_{-} component is time independent and is given by

$$H_{-} = \tfrac{1}{2}I_j^{-}\omega_{\text{nut}}\exp\{-i(\psi_p + \phi_{\text{frame}})\} + \tfrac{1}{2}I_j^{+}\omega_{\text{nut}}\exp\{+i(\psi_p + \phi_{\text{frame}})\} \text{ (for } \gamma > 0). \qquad [33]$$

In the case of *negative* γ, the H_{+} component is time independent and is given by

$$H_{+} = \tfrac{1}{2}I_j^{-}\omega_{\text{nut}}\exp\{+i(\psi_p - \phi_{\text{frame}})\} + \tfrac{1}{2}I_j^{+}\omega_{\text{nut}}\exp\{-i(\psi_p - \phi_{\text{frame}})\} \text{ (for } \gamma < 0). \qquad [34]$$

In both cases, the ''counterrotating'' components (H_{+} in the case of $\gamma > 0$ and H_{-} in the case $\gamma < 0$) are rapidly time dependent, and to a good approximation only give rise to small Bloch–Siegert shifts (*21*), which may usually be ignored.

I now consider the sense of the nutation frequency ω_{nut}. From Eq. [25], the nutation frequency ω_{nut} is negative for the case of positive γ spins, and positive for the case of negative γ spins. This implies that positive γ spins precess in the clockwise direction around the rotating-frame fields, while negative γ spins precess in the anticlockwise direction.

In this article, I adopt the usage of Ernst and co-workers (*22*), in which the sign of ω_{nut} is deliberately cancelled by a proper choice of the rotating-frame phase ϕ_{frame}:

$$\phi_{\text{frame}} = \begin{cases} \pi & \text{if } \gamma > 0 \\ 0 & \text{if } \gamma < 0 \end{cases} \qquad [35]$$

This compensates for the awkward change in sign of the nutation frequency ω_{nut} for spins with opposite signs of γ and ensures that strong ideal pulses of flip angle β always lead to mathematically positive rotations of the spin polarizations through the angle β in the rotating frame. However, I emphasize that this ''positive nutation'' convention is independent of the rest of this article. The conclusions as to the sense of the RF phase shift hold whatever the convention for the sense of the nutation.

With the choice of ϕ_{frame} given in Eq. [35], the resonant component of the rotating-frame spin Hamiltonian is

$$H_{-} = \tfrac{1}{2}I_j^{-}|\omega_{\text{nut}}|\exp\{-i\psi_p\} + \tfrac{1}{2}I_j^{+}|\omega_{\text{nut}}|\exp\{i\psi_p\} \quad (\text{for } \gamma > 0), \qquad [36]$$

and

$$H_{+} = \tfrac{1}{2}I_j^{-}|\omega_{\text{nut}}|\exp\{i\psi_p\} + \tfrac{1}{2}I_j^{+}|\omega_{\text{nut}}|\exp\{-i\psi_p\} \quad (\text{for } \gamma < 0). \qquad [37]$$

I now introduce the *phase of the nutation axis* ϕ_p, which is related to the phase of the RF carrier wave during the pulse according to

$$\phi_p = -(\text{sign } \gamma)\psi_p. \qquad [38]$$

The rotating-frame spin Hamiltonian during the pulse may then be cast in a γ-independent form

$$H \cong \Delta\omega_0^j I_{jz} + |\omega_{\rm nut}|(I_{jx}\cos\phi_p + I_{jy}\sin\phi_p), \quad [39]$$

where $\Delta\omega_0^j$ is the resonance offset (ignoring the Bloch–Siegert shift):

$$\Delta\omega_0^j = \omega_0^j - \omega_{\rm frame}, \quad [40]$$

and $|\omega_{\rm nut}|$ is the magnitude of the nutation frequency.

Equation [39] is the familiar form of the rotating-frame Hamiltonian, corresponding to the nutation of the spins about an axis with a longitudinal z component proportional to the resonance offset and a transverse component proportional to the radiofrequency field. The only new feature is that the orientation of the nutation axis in the transverse plane is set by the phase angle ϕ_p, which is opposite in sign to the electronic phase shift ψ_p of the RF carrier wave for spins of positive γ (Eq. [38] and Fig. 2).

For positive γ, the phase shift of the nutation axis is opposite in sign to the values shown in current pulse programs. For example, programming the RF carrier phase as $\psi_p = \pi/2$ (generally called a ''y pulse'') nutates positive γ spins about an axis with phase $\phi_p = -\pi/2$ (the $-y$ axis for strong RF pulses). Similarly, programming the RF carrier phase phase as $\psi_p = 3\pi/2$ (generally called a ''$-y$ pulse'') nutates positive γ spins about an axis with phase $\phi_p = +\pi/2$ (the y axis for strong RF pulses). Pulses of phase $\psi_p = 0$ and $\psi_p = \pi$, on the other hand, come out ''right,'' in the sense that the nutation is about the expected axis (the x axis for strong pulses of phase $\psi_p = 0$ and the $-x$ axis for strong pulses of phase $\psi_p = \pi$).

The dynamics of nuclear spins are sensitive to the sense of the nutation axis phase shift. All pulse sequences involving phase shifts in noninteger multiples of π must take into account the direction of the nutation axis in order to obtain correct physical predictions. A simple example is given later.

These conclusions are independent of the sense of the nutation *around* the rotating-frame axes. If the phase angle $\phi_{\rm frame}$ is set to zero, the sign of the nutation frequency $\omega_{\rm nut}$ is retained. The same conclusions apply, but with an uniform π phase shift of *all* nutation axes, in the case of positive γ. Since the NMR experiment is only sensitive to *relative* phase shifts, this does not matter.

It is quite surprising that the above problem seems not to have attracted notice earlier. As argued below, this may be because of another common sign error in the labeling of the spectral frequency coordinate.

THE NMR SIGNAL

Spin Coherences

The relationship between the spin coherences and the time-domain signal (free-induction decay) is now examined. For simplicity, an ensemble of isolated spins-$\frac{1}{2}$ in equivalent sites j with Larmor frequency ω_0^j is considered.

The laboratory-frame density operator for the spin ensemble may be written

$$\rho^L = \rho^L_{\boxminus} I_j^- + \rho^L_{\boxplus} I_j^+ + \rho^L_{\boxed{\alpha}} I_j^\alpha + \rho^L_{\boxed{\beta}} I_j^\beta, \quad [41]$$

with the following abbreviations for the spin-state populations and the laboratory-frame (± 1)-quantum coherences:

$$\begin{aligned}
\rho^L_{\boxminus} &= \langle\beta|\rho^L|\alpha\rangle \\
\rho^L_{\boxplus} &= \langle\alpha|\rho^L|\beta\rangle = \rho^L_{\boxminus}{}^* \\
\rho^L_{\boxed{\alpha}} &= \langle\alpha|\rho^L|\alpha\rangle \\
\rho^L_{\boxed{\beta}} &= \langle\beta|\rho^L|\beta\rangle = 1 - \rho^L_{\boxed{\alpha}}.
\end{aligned} \quad [42]$$

The laboratory-frame spin-density operator obeys the von Neumann equation of motion

$$\frac{d}{dt}\rho^L(t) = -i[H^L(t), \rho^L(t)] - \hat{\hat{\Gamma}}\rho^L(t), \quad [43]$$

where H^L is the coherent part of the spin Hamiltonian and $\hat{\hat{\Gamma}}$ is the relaxation superoperator in the Redfield limit [including thermal polarization effects if desired, see Ref. (*8, 9*)]. If there are no RF fields, and under the usual ''secular'' approximations for the relaxation, the free precessional motion of the laboratory-frame coherences from time point t_a to a later time t_b is

$$\begin{aligned}
\rho^L_{\boxminus}(t_b) &= \rho^L_{\boxminus}(t_a)\exp\{(i\omega_0^j - \lambda)(t_b - t_a)\} \\
\rho^L_{\boxplus}(t_b) &= \rho^L_{\boxplus}(t_a)\exp\{(-i\omega_0^j - \lambda)(t_b - t_a)\}.
\end{aligned} \quad [44]$$

Here $\lambda = T_2^{-1}$ is the damping rate constant for the (± 1)-quantum coherences (''spin–spin relaxation rate''). The (-1)-quantum coherence $\rho^L_{\boxminus}$ rotates in the complex plane at the Larmor frequency ω_0^j, while the $(+1)$-quantum coherence $\rho^L_{\boxplus}$ rotates in the complex plane in the opposite sense, at the frequency $-\omega_0^j$. The physical precession of the spin magnetization vector in the transverse plane corresponds to the abstract motion of the (-1)-quantum coherence in the complex plane.

The rotating-frame spin-density operator is given by

$$\rho(t) = V(t)^\dagger \rho^L(t) V(t), \quad [45]$$

where the transformation operator $V(t)$ is given by Eq. [29]. The rotating-frame density operator may be written

$$\rho = \rho_{\boxminus} I_j^- + \rho_{\boxplus} I_j^+ + \rho_{\boxed{\alpha}} I_j^\alpha + \rho_{\boxed{\beta}} I_j^\beta \quad [46]$$

and obeys the equation of motion

$$\frac{d}{dt}\rho(t) = -i[H(t), \rho(t)] - \hat{\hat{\Gamma}}\rho(t), \quad [47]$$

where H is the rotating-frame spin Hamiltonian given in Eq. [39]. The rotating-frame and laboratory-frame coherences and populations are related through

$$\begin{aligned}\rho_{\boxminus}(t) &= \rho^L_{\boxminus}(t)\exp\{-i(\omega_{\text{frame}}t + \phi_{\text{frame}})\}\\ \rho_{\boxplus}(t) &= \rho^L_{\boxplus}(t)\exp\{+i(\omega_{\text{frame}}t + \phi_{\text{frame}})\}\\ \rho_{\boxed{\alpha}}(t) &= \rho^L_{\boxed{\alpha}}(t)\\ \rho_{\boxed{\beta}}(t) &= \rho^L_{\boxed{\beta}}(t).\end{aligned} \quad [48]$$

The free precessional motion of the rotating-frame (± 1)-quantum coherences in the absence of applied RF fields is therefore

$$\begin{aligned}\rho_{\boxminus}(t_b) &= \rho_{\boxminus}(t_a)\exp\{(i\Delta\omega^j_0 - \lambda)(t_b - t_a)\}\\ \rho_{\boxplus}(t_b) &= \rho_{\boxplus}(t_a)\exp\{(-i\Delta\omega^j_0 - \lambda)(t_b - t_a)\},\end{aligned} \quad [49]$$

where $\Delta\omega^j_0$ is the resonance offset (Eq. [40]).

The (-1)-quantum rotating-frame coherence $\rho_{\boxminus}$ rotates in the complex plane at the resonance offset frequency $\Delta\omega^j_0$, while the $(+1)$-quantum rotating-frame coherence $\rho_{\boxplus}$ rotates in the complex plane in the opposite sense, at the frequency $-\Delta\omega^j_0$.

The motion of the (-1)-quantum rotating-frame coherence $\rho_{\boxminus}$ in the complex plane corresponds exactly to the physical precession of the transverse spin magnetization in the rotating frame. On quadrature detection, signals induced by the (-1)-quantum rotating-frame coherences may therefore be regarded as ''true'' NMR peaks, while signals associated with $(+1)$-quantum rotating-frame coherences are ''quadrature artifacts,'' rotating at minus the resonance offset and appearing at mirror image positions in the spectrum. A well-adjusted quadrature receiver selects the (-1)-quantum signals and suppresses the $(+1)$-quantum artifacts. Note that this interpretation is independent of the sign of γ.

The Free-Induction Decay

I now examine the connection between the radiofrequency NMR signal and the single-quantum coherences of the nuclear spin system. Suppose that the RF coil is located along the x axis of the laboratory system. The nuclear spin magnetization along the x axis is proportional to the nuclear spin angular momentum and is given by

$$\begin{aligned}M_x &\sim \langle I_{jx}\rangle\\ &= \text{Tr}\{\rho^L I_{jx}\}\\ &\sim \rho^L_{\boxminus} + \rho^L_{\boxplus},\end{aligned} \quad [50]$$

omitting unnecessary constants. Obviously, the laboratory-frame $(+1)$- and (-1)-quantum coherences both contribute to the transverse nuclear spin magnetization.

If the sample is static or the RF field perfectly uniform, the phase modulation effects described by Goldman *et al.* (*14*) and others (*15, 16*) may be ignored. The voltage generated in the coil is proportional to the time derivative of the nuclear spin magnetization in the coil direction. Assuming that the free-induction decay is simply proportional to this voltage and ignoring constant instrumental phase shifts, I get

$$\begin{aligned}s_{\text{FID}}(t) &\sim \frac{d}{dt}M_x\\ &\sim \frac{d}{dt}\rho^L_{\boxminus}(t) + \frac{d}{dt}\rho^L_{\boxplus}(t).\end{aligned} \quad [51]$$

This corresponds to

$$\begin{aligned}s_{\text{FID}}(t) \sim\ & +i\omega_{\text{frame}}\rho_{\boxminus}(t)\exp\{+i(\omega_{\text{frame}}t + \phi_{\text{frame}})\}\\ & -i\omega_{\text{frame}}\rho_{\boxplus}(t)\exp\{-i(\omega_{\text{frame}}t + \phi_{\text{frame}})\},\end{aligned} \quad [52]$$

ignoring the slow time dependence of the rotating-frame coherences $\rho_{\boxminus}$ and $\rho_{\boxplus}$. Substitution of Eq. [30] and Eq. [35] leads to the following relationship between the FID and the rotating-frame coherences:

$$\begin{aligned}s_{\text{FID}}(t) \sim\ & +i|\omega^{\text{carrier}}|\rho_{\boxminus}(t)\exp\{+i\omega_{\text{frame}}t\}\\ & -i|\omega^{\text{carrier}}|\rho_{\boxplus}(t)\exp\{-i\omega_{\text{frame}}t\}.\end{aligned} \quad [53]$$

The multiplicative factor $|\omega^{\text{carrier}}|$ is now dropped for simplicity, after noting that the efficiency of signal induction is approximately proportional to the Larmor frequency, as it should be.

Quadrature Detection

Quadrature detection of the NMR signal is now considered, in particular the connection between the digitized NMR signal and the rotating-frame coherences of the spin system. For simplicity, a traditional two-channel quadrature receiver is considered. More sophisticated detection schemes, involving signal oversampling and digital signal processing, are common, but the basic principles are not very different.

A block diagram of a traditional quadrature receiver is shown in Fig. 3. The signal flow is from left to right. The receiver receives two inputs, the amplified free-induction decay s_{FID} and the receiver reference signal s_{rec}. Both of these input signals are split and directed down two equivalent paths. The split receiver reference signals are given a relative phase shift of $\pi/2$. The NMR signals and receiver reference signals are multiplied together by RF mixers and subjected to low-pass filtration. The audio analogue outputs of the two low pass filters are denoted s_{A} and s_{B}.

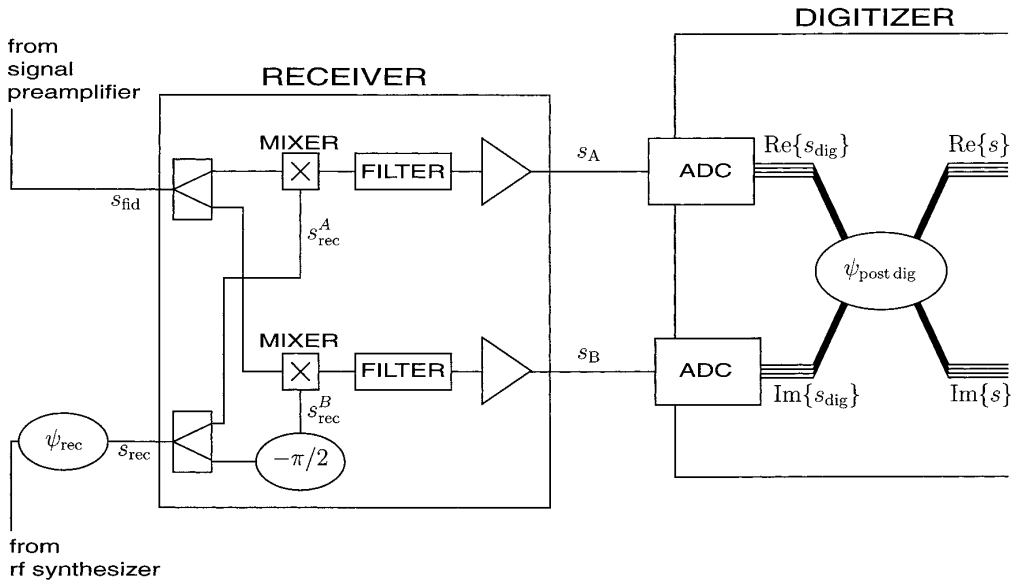

FIG. 3. A block diagram of a conventional quadrature receiver and the subsequent digitization stage. The oval symbols denote phase shifts.

The RF receiver reference signal is proportional to

$$s_{\rm rec}(t) \sim 2\cos(|\omega^{\rm carrier}|t + \psi_{\rm rec}), \qquad [54]$$

where $\psi_{\rm rec}$ is the radiofrequency receiver reference phase, usually under pulse program control. The carrier phase $|\omega^{\rm carrier}|$ during signal detection is usually the same as that used under the excitation pulse sequence, but this is not essential. As usual, the symbol ψ indicates that no account is yet taken of the sign of γ.

The receiver outputs are digitized by separate ADCs. The two ADC outputs are subsequently treated as the real and imaginary components of a complex digital signal, denoted here $s_{\rm dig}$. If the output of channel A is assigned as the real part, and the output of channel B is assigned as the imaginary part, the digitized complex NMR signal is given by

$$s_{\rm dig}(t) = s_{\rm A}(t) + is_{\rm B}(t). \qquad [55]$$

The quadrature NMR signal $s_{\rm dig}(t)$ is generally given a further phase shift after digitization, before co-addition with the accumulated NMR signals of previous signal acquisitions. On many instruments, this phase shift is implemented by hardwired manipulations of the outputs of the ADCs and may be expressed mathematically

$$s(t) = s_{\rm dig}(t)\exp\{i\psi_{\rm post\,dig}\}, \qquad [56]$$

where $s(t)$ is the complex digitized NMR signal transferred to the computer. For example, a post-digitization phase shift of $\psi_{\rm post\,dig} = \pi/2$ corresponds to the following relationship of the real and imaginary parts of the signals:

$$\begin{aligned}\mathrm{Re}\{s(t)\} &= -\mathrm{Im}\{s_{\rm dig}(t)\}\\ \mathrm{Im}\{s(t)\} &= +\mathrm{Re}\{s_{\rm dig}(t)\}.\end{aligned} \qquad [57]$$

This may therefore be implemented by swapping the outputs of the real and imaginary channels, followed by a change in sign of the real channel. Phase shifts of $\psi_{\rm post\,dig} = \pi$ and $3\pi/2$ may be executed in similar fashion. Although post-digitization phase shifts in multiples of $2\pi/3$ have advantages (*23*), current instruments are usually only capable of easily implementing values of $\psi_{\rm post\,dig}$ in multiples of $\pi/2$.

The post-digitization phase shift $\psi_{\rm post\,dig}$ is often confused with the radiofrequency receiver reference phase $\psi_{\rm rec}$. These phases are actually completely distinct. For example, signals with different RF phases and post-digitization phase shifts $\psi_{\rm post\,dig}$ may be combined, in order to remove artifacts caused by imbalance in the quadrature receiver channels (*24*). This effect cannot be achieved by cycling of the radiofrequency phases $\phi_{\rm rec}$.

The connection is now traced among the radiofrequency FID $s_{\rm FID}$, the spin coherences, and the digitized signal $s(t)$, keeping careful track of relative signs. For simplicity, the two channels of the quadrature receiver are assumed to have identical electrical characteristics. The two receiver reference signals at the inputs to the mixers are taken as

$$\begin{aligned}s^{\rm A}_{\rm rec}(t) &\sim 2\cos(|\omega^{\rm carrier}|t + \psi_{\rm rec})\\ s^{\rm B}_{\rm rec}(t) &\sim 2\cos\left(|\omega^{\rm carrier}|t + \psi_{\rm rec} - \frac{\pi}{2}\right).\end{aligned} \qquad [58]$$

This corresponds to an overall RF receiver phase shift of ψ_{rec} and a relative phase shift of $\pi/2$ between the two channels. The sign of the relative phase shift between the two channels is fixed internally in the receiver hardware. As seen below, the relative phases in Eq. [58] are compatible with the assignment of the ''A'' and ''B'' channel outputs to the real and imaginary parts of a complex NMR signal.

The output of mixer A is proportional to the product of the inputs and is given by $s_{\mathrm{FID}}(t)s^{\mathrm{A}}_{\mathrm{rec}}(t)$. A similar equation applies to the output of mixer B. The two mixer outputs are subjected to low-pass electronic filtration, which may be expressed mathematically as a convolution with a time-domain filter function:

$$\begin{aligned} s_{\mathrm{A}}(t) &\sim [s_{\mathrm{FID}}(t)s^{\mathrm{A}}_{\mathrm{rec}}(t)] \otimes g(t) \\ s_{\mathrm{B}}(t) &\sim [s_{\mathrm{FID}}(t)s^{\mathrm{B}}_{\mathrm{rec}}(t)] \otimes g(t). \end{aligned} \quad [59]$$

The convolution is defined (*25*)

$$f(t) \otimes g(t) = \int_{-\infty}^{\infty} f(t')g(t' - t)dt', \quad [60]$$

where $g(t)$ is a smooth time-domain function which changes little on the time scale of a single period of the carrier frequency $|\omega^{\mathrm{carrier}}|$. The effect of the time-domain convolution is to remove radiofrequency components of the input function.

The digitized complex NMR signal is given by

$$s_{\mathrm{dig}}(t) = s_{\mathrm{A}}(t) + is_{\mathrm{B}}(t). \quad [61]$$

Since convolution is a linear operation, the digitized complex NMR signal at the outputs of the ADCs is given by

$$\begin{aligned} s_{\mathrm{dig}}(t) &= s_{\mathrm{A}}(t) + is_{\mathrm{B}}(t) \\ &= [s_{\mathrm{FID}}(t)(s^{\mathrm{A}}_{\mathrm{rec}}(t) + is^{\mathrm{B}}_{\mathrm{rec}}(t))] \otimes g(t) \\ &= [2s_{\mathrm{FID}}(t)\exp\{i(|\omega^{\mathrm{carrier}}|t + \psi_{\mathrm{rec}})\}] \otimes g(t). \end{aligned} \quad [62]$$

Inclusion of the post-digitization phase shift leads to the following form of the complex NMR signal as represented in the computer:

$$\begin{aligned} s(t) = [2s_{\mathrm{fid}}(t)\exp\{i(|\omega^{\mathrm{carrier}}|t + \psi_{\mathrm{rec}} + \psi_{\mathrm{post\ dig}})\}] \\ \otimes g(t). \end{aligned} \quad [63]$$

It proves useful to define a γ-sensitive receiver reference phase ϕ_{rec} and post-digitization phase $\phi_{\mathrm{post\ dig}}$, with the same relationship to the raw phases ψ_{rec} and $\psi_{\mathrm{post\ dig}}$ as holds for the pulse phases ψ_p and ϕ_p (Eq. [38]):

$$\begin{aligned} \phi_{\mathrm{rec}} &= -(\mathrm{sign}\ \gamma)\psi_{\mathrm{rec}} \\ \phi_{\mathrm{post\ dig}} &= -(\mathrm{sign}\ \gamma)\psi_{\mathrm{post\ dig}}. \end{aligned} \quad [64]$$

The complex NMR signal may then be written

$$\begin{aligned} s(t) = [2s_{\mathrm{FID}}(t)\exp\{-i(\mathrm{sign}\ \gamma) \\ \times (\omega_{\mathrm{frame}}t + \phi_{\mathrm{rec}} + \phi_{\mathrm{post\ dig}})\}] \otimes g(t). \end{aligned} \quad [65]$$

This may be combined with Eq. [53] to obtain the desired explicit link between the rotating-frame spin coherences and the digitized NMR signal. For positive γ nuclei, one obtains

$$\begin{aligned} s(t) \sim 2i\rho_{\boxminus}(t)\exp\{-i(\phi_{\mathrm{rec}} + \phi_{\mathrm{post\ dig}})\} \\ (\mathrm{for}\ \gamma > 0), \end{aligned} \quad [66]$$

while for negative γ nuclei, a different equation is obtained

$$\begin{aligned} s(t) \sim -2i\rho_{\boxplus}(t)\exp\{+i(\phi_{\mathrm{rec}} + \phi_{\mathrm{post\ dig}})\} \\ (\mathrm{for}\ \gamma < 0). \end{aligned} \quad [67]$$

To obtain these equations, the convolution with the filter function $g(t)$ was taken into account by removing all high-frequency signal components.

For positive γ nuclei, Eq. [66] reveals the expected relationship between the rotating-frame (-1)-quantum coherences and the detected signal. As remarked above, the rotation of the (-1)-quantum coherences in the complex plane has a direct correspondence with the precession of the transverse spin magnetization in the rotating frame. For negative γ nuclei, on the other hand, the relationship Eq. [67] is ''backward,'' in the sense that the NMR signal is related to the $(+1)$-quantum coherences. This means that for negative γ nuclei, a normal quadrature receiver actually detects the quadrature artifacts, rotating in the mirror-image sense in the rotating frame. Physically this is because at present (i) the receiver channels are hardwired in a fixed phase relationship, and (ii) the assignment of the receiver outputs to the real and imaginary components of the complex signal takes no account of the sense of the Larmor frequency.

One of the recommendations of this article is that this problem is rectified by taking the *complex conjugate* of the digital signal, in the case of negative γ. The above equation then becomes

$$\begin{aligned} s(t)^* \sim 2i\rho_{\boxminus}(t)\exp\{-i(\phi_{\mathrm{rec}} + \phi_{\mathrm{post\ dig}})\} \\ (\mathrm{for}\ \gamma < 0). \end{aligned} \quad [68]$$

The right-hand side of this equation has the same form as the equation for positive γ nuclei. The physical significance of taking the complex conjugate is to reverse the relative phase shift of the two receiver channels, reflecting the different senses of the Larmor precession. This could also be done by hardware, but a software solution is probably more convenient.

In order to elucidate the interplay of these phases, consider a simple experiment in which a strong $\pi/2$ pulse is applied with rotating-frame field phase ϕ_p, followed by signal detection using a receiver phase ϕ_{rec}, and post-digitization processing of the NMR signals with the phase shift $\phi_{\mathrm{post\,dig}}$. The discussion will be conducted using the γ-sensitive phases ϕ rather than the ''absolute'' phases ψ.

If the pulse has flip angle $\pi/2$, its duration is $\tau_p = (\pi/2)/|\omega_{\mathrm{nut}}|$. Signal acquisition is supposed to begin immediately after the pulse. The initial spin-density operator is assumed to be in thermal equilibrium

$$\rho(-\tau_p) \sim I_{jz}, \qquad [69]$$

omitting unnecessary constants. During the pulse, the spin system experiences a rotating-frame Hamiltonian given by Eq. [39], which may be written

$$H \cong |\omega_{\mathrm{nut}}| R_{jz}(\phi_p) I_{jx} R_{jz}(-\phi_p), \qquad [70]$$

where R_{jz} is the operator for rotations of spins I_j around the z axis:

$$R_{jz}(\phi_p) = \exp\{-i\phi_p I_{jz}\}. \qquad [71]$$

The resonance offset is ignored during the strong pulse, for simplicity. The pulse produces a spin-density operator given by

$$\begin{aligned}\rho(0) &= \exp\{-iH\tau_p\}\rho(-\tau_p)\exp\{+iH\tau_p\} \\ &\sim -R_{jz}(\phi_p) I_{jy} R_{jz}(-\phi_p),\end{aligned} \qquad [72]$$

assuming a pulse with flip angle $|\omega_{\mathrm{nut}}|\tau_p = \pi/2$. The rotating-frame (± 1)-quantum coherences at the beginning of signal acquisition (time point $t = 0$) are given by

$$\begin{aligned}\rho_{\boxminus}(0) &\sim \frac{1}{2i}\exp\{i\phi_p\} \\ \rho_{\boxplus}(0) &\sim -\frac{1}{2i}\exp\{-i\phi_p\}.\end{aligned} \qquad [73]$$

This shows that the (-1)-quantum coherence picks up a phase factor equal to the nutation axis phase ϕ_p, while the $(+1)$-quantum coherence picks up an opposite phase factor.

If free evolution now takes place in the absence of applied RF fields, I get the following equations for the rotating-frame coherences at times $t \geqslant 0$:

$$\begin{aligned}\rho_{\boxminus}(t) &= \frac{1}{2i}\exp\{i(\Delta\omega_0^j t + \phi_p) - \lambda t\} \\ \rho_{\boxplus}(t) &= -\frac{1}{2i}\exp\{-i(\Delta\omega_0^j t + \phi_p) - \lambda t\}.\end{aligned} \qquad [74]$$

Consider now the case of $\gamma > 0$. The final signal, after quadrature detection, digitization, and post-digitization phase shifting, is given by

$$s(t) \sim \exp\{i(\Delta\omega_0^j t + \phi^{\mathrm{tot}}) - \lambda t\} \text{ (for } \gamma > 0), \qquad [75]$$

where the total signal phase shift is

$$\phi^{\mathrm{tot}} = \phi_p - \phi_{\mathrm{rec}} - \phi_{\mathrm{post\,dig}}. \qquad [76]$$

In terms of the electronic carrier phase shifts and the absolute post-digitization phase shift, this may be written

$$\phi^{\mathrm{tot}} = -\psi_p + \psi_{\mathrm{rec}} + \psi_{\mathrm{post\,dig}} \text{ (for } \gamma > 0). \qquad [77]$$

Several observations may now be made:

1. The NMR signal is insensitive to identical RF phase shifts of the pulse and the receiver.
2. If the receiver is perfectly adjusted, the receiver reference phase ϕ_{rec} and post-digitization phase shift $\phi_{\mathrm{post\,dig}}$ behave identically.
3. NMR signals accumulate if the total phase ϕ^{tot} is the same on every transient. For example, if the receiver reference phase during the signal detection is set to zero ($\phi_{\mathrm{rec}} = 0$), then signals accumulate if the nutation axis phase ϕ_p and the γ-sensitive post-digitization phase $\phi_{\mathrm{post\,dig}}$ are always equal. This corresponds to the well-known CYCLOPS procedure for canceling the effects of receiver imperfections (*24*). The phases ϕ_p and $\phi_{\mathrm{post\,dig}}$ increment synchronously in steps of $\pi/2$.
4. Current implementations of CYCLOPS manipulate the absolute carrier phase of the pulse ψ_p and the absolute post-digitization phase shift $\psi_{\mathrm{post\,dig}}$. As *both* of these are related to the γ-sensitive phases ϕ_p and $\phi_{\mathrm{post\,dig}}$ through a sign change, current implementations of CYCLOPS do of course work properly.

For negative γ nuclei, similar conclusions apply. According to Eq. [67], the NMR signal is given by

$$s(t) \sim \exp\{-i(\Delta\omega_0^j t + \phi^{\mathrm{tot}}) - \lambda t\} \text{ (for } \gamma < 0), \qquad [78]$$

where the total signal phase shift is

$$\begin{aligned}\phi^{\mathrm{tot}} &= \phi_p - \phi_{\mathrm{rec}} - \phi_{\mathrm{post\,dig}} \\ &= \psi_p - \psi_{\mathrm{rec}} - \psi_{\mathrm{post\,dig}} \text{ (for } \gamma < 0).\end{aligned} \qquad [79]$$

The total signal phase shifts for nuclei of positive and negative γ differ only by a sign change. Since phase-cycling procedures such as CYCLOPS are designed to give zero overall phase shift for desired coherence-transfer pathways, they work identically for positive and negative γ nuclei.

This article recommends taking the complex conjugate of

the digitized signals from negative γ nuclei. In this case, the NMR signal in a single-pulse experiment is

$$s(t)^* \sim \exp\{+i(\Delta\omega_0^j t + \phi^{\text{tot}}) - \lambda t\} \text{ (for } \gamma < 0). \quad [80]$$

The digitized signal $s(t)^*$ from negative γ nuclei has an identical form to the digitized signal $s(t)$ from positive γ nuclei. Selective use of the complex conjugate allows experiments to be treated consistently for all nuclei. I return to this point below.

FOURIER TRANSFORMATION AND THE NMR SPECTRUM

Spins of Positive Magnetogyric Ratio

I first discuss the processing of NMR signals from spins with positive γ. The digitized, accumulated, NMR signal is subjected to numerical Fourier transformation, defined

$$S(\omega) = \int_0^\infty s(t)\exp\{-i\omega t\}\,dt. \quad [81]$$

This equation implies that the time origin $t = 0$ is chosen to be the start of signal detection. The technical differences between discrete and continuous Fourier transforms are ignored.

For the simple one-pulse experiment described above, the contribution of one FID to the spectrum is easily evaluated as

$$S(\omega) \sim \exp\{i\phi^{\text{tot}}\}L(\omega;\, \Delta\omega_0^j,\, \lambda), \quad [82]$$

where the combined phase shift ϕ^{tot} of the excitation and detection processes is given in Eq. [76]. The complex Lorentzian peakshape function is defined

$$L(\omega;\, \omega_{\text{center}},\, \lambda) = \frac{1}{\lambda + i(\omega - \omega_{\text{center}})}. \quad [83]$$

The real part of $L(\omega;\, \omega_{\text{center}},\, \lambda)$ is an ''absorption'' Lorentzian centered at the frequency ω_{center} and with half-width-at-half-height λ. The imaginary part is minus a ''dispersion'' Lorentzian

$$L = A - iD. \quad [84]$$

The question now arises as to how the spectrum $S(\omega)$ should be presented, so as to conform to the accepted convention for the display of chemical-shift information.

The universal convention for the presentation of NMR spectra is that least-shielded resonances are shown on the left of the spectrum, while most-shielded resonances appear on the right. The σ scale (shielding) increases from left to right, and the δ scale (deshielding) increases from right to left. This venerable convention originates in the days of field-swept NMR, where the applied magnetic field was plotted as increasing from left to right across the spectrum.

As shown above, the peaks in the NMR spectrum of uncoupled spins appear at the chemically shifted resonance offset frequencies $\Delta\omega_0^j = \omega_0^j - \omega_{\text{frame}}$, where ω_{frame} is the frequency of the rotating frame, equal to minus the spectrometer carrier frequency $|\omega^{\text{carrier}}|$. The resonance offset of an isolated spin with shielding constant σ^j is given by

$$\Delta\omega_0^j = \omega_0(1 - \sigma^j) - \omega_{\text{frame}}, \quad [85]$$

which is conveniently written

$$\Delta\omega_0^j = -\omega_0(\sigma^j - \sigma^0). \quad [86]$$

Here σ^0 is the rotating-frame frequency (the center of the spectrum), expressed in shielding units. In deshielding units, the same resonance offset frequency may be written

$$\Delta\omega_0^j = \omega_0(\delta^j - \delta^0), \quad [87]$$

where δ^0 is the rotating-frame frequency (the center of the spectrum) on the deshielding scale.

The Larmor frequency ω_0 is negative for spins of positive γ. It follows that well-shielded spins (high values of σ^j) are shifted to positive frequency, while less-shielded spins (low values of σ^j) are shifted to negative frequency. Since spectra are presented with shielding increasing from left to right, the correct presentation of the function $S(\omega)$ is with negative frequency coordinates $\omega < 0$ on the left, positive frequency coordinates $\omega > 0$ on the right, and zero frequency $\omega = 0$ at the center. The spectral function $S(\omega)$ produced by Fourier transformation of the signal $s(t)$ should therefore be plotted and labeled in the usual mathematical convention, with the frequency axis increasing from left to right, as shown in Fig. 4.

Plotted this way, the frequency coordinate of a NMR peak corresponds directly to the precession frequency of the magnetization in the rotating frame. Spectral peaks in the right-hand half of the spectrum are associated with magnetization components precessing in the positive (anticlockwise) direction in the rotating frame. Spectral peaks in the left-hand half of the spectrum are associated with magnetization components of less-well-shielded sites, which precess in the negative (clockwise) direction in the rotating frame. Spectral peaks at the center of the spectrum ($\omega = 0$) are associated with magnetization components whose precession frequency exactly matches the rotating-frame frequency.

The above recommendations for plotting the *function* $S(\omega)$ correspond to actual practice on current instruments. However, usually, the *frequency axis labeling is reversed.*

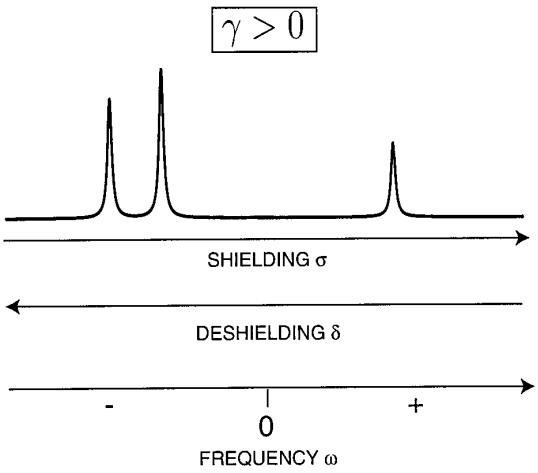

FIG. 4. Frequency axes for nuclei with positive magnetogyric ratio. By tradition, the shielding scale σ increases from left to right, while the deshielding scale δ increases from right to left. The origin of these scales is set by agreed reference compounds. The spectral frequency coordinate ω increases from left to right, with zero corresponding to the Larmor frequency $\omega_0 = \omega_{\rm frame} = -|\omega^{\rm carrier}|$. The plotted spectral function is $S(\omega)$ (Eq. [81]).

On commercial instruments, the spectral function $S(\omega)$ is plotted as described above, but the frequency axis is usually labeled *as if* negative frequencies were on the right, and positive frequencies were on the left. This corresponds to a labeling of the axis with the corresponding value of $|\omega_0^j| - |\omega^{\rm carrier}|$, which actually corresponds to minus the true frequency coordinate, in the case of positive γ nuclei. Note that it is only the labeling which is incorrect, not the sense of the plotted function $S(\omega)$. This would merely be an irritating mistake, if it had not also contributed to a misinterpretation of the sense of rotating-frame precession of the spins. This has in turn obscured the simultaneous error in the sense of the nutation axis phase shift. Seen in isolation, these errors cancel and are not disturbing. However, they lead to awkward difficulties in a wider context, when the signs of spin interactions are related to particular spectral features.

Spins of Negative Magnetogyric Ratio

The signal processing and spectral presentation for spins with negative γ is subject to even more serious confusion.

As discussed above, it is recommended that the complex conjugate of the digitized signal $s(t)$ is taken before Fourier transformation. I first discuss the situation *without* implementation of the complex conjugate, i.e., the *status quo* on current instruments.

The current practice is to process the signals from negative-γ nuclei in identical fashion to the signals from positive-γ nuclei. For isolated negative-γ spins in sites j, Fourier transformation (Eq. [81]) of the signal (Eq. [78]) yields the spectral function

$$S(\omega) \sim \exp\{-i\phi^{\rm tot}\} L(\omega; -\Delta\omega_0^j, \lambda) \text{ (for } \gamma < 0), \quad [88]$$

where the overall phase shift $\phi^{\rm tot}$ from the excitation and detection processes is given in Eq. [79]. Note that the Lorentzian peak appears at *minus* the resonance offset $\Delta\omega_0^j$. This is a ''quadrature image'' of the real NMR peak, consistent with the observation of $(+1)$-quantum rotating-frame coherences for negative-γ nuclei.

We must now reconsider how to present this spectrum, so as to be consistent with the conventional chemical-shift scale. Since the Larmor frequency is positive, well-shielded spins (high values of σ^j) are shifted to negative frequency, while less-shielded spins (low values of σ^j) are shifted to positive frequency. It follows that the resonance offset $\Delta\omega_0^j$ increases from right to left for negative-γ nuclei. This is illustrated in Fig. 5.

This would seem to imply that for negative γ, the spectrum should be plotted backward, with the ω-coordinate increasing from right to left. However, since the conventional procedure detects the quadrature images, spectral peaks actually appear at the mirror-image frequencies $-\Delta\omega_0^j$. As a result, a conventionally oriented spectrum is achieved by plotting the spectrum $S(\omega)$ in the usual mathematical sense, with the frequency coordinate increasing from left to right. To add to the confusion, the frequency axis is then labeled according to the corresponding value of $|\omega_0^j| - |\omega^{\rm carrier}|$, which increases from right to left, and which now has a very distant relationship with the rotating-frame precession frequencies of the magnetization components.

It is not easy to pick one's way through this confusion. Fortunately, there is an easy way out. Define the spectral function $\bar{S}$ as the Fourier transform of the *complex conjugate* of the time-domain signal $s(t)$:

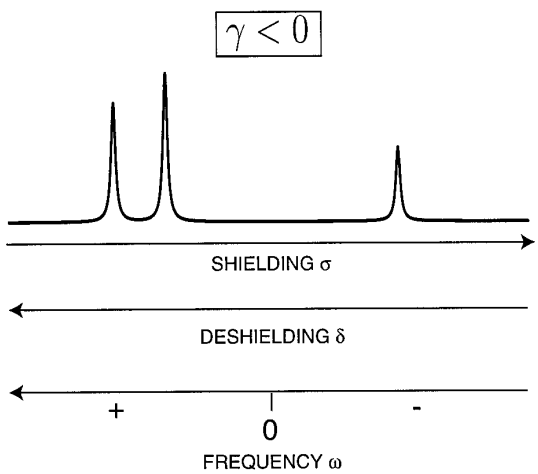

FIG. 5. Frequency axes for nuclei with negative magnetogyric ratio. The spectral frequency coordinate ω increases from right to left, with zero corresponding to the Larmor frequency $\omega_0 = \omega_{\rm frame} = +|\omega^{\rm carrier}|$. The plotted spectral function $\bar{S}(\omega)$ is the Fourier transform of the complex conjugate of the time-domain signal (Eq. [89]).

$$\bar{S}(\omega) = \int_0^\infty s(t)^* e^{-i\omega t} dt. \qquad [89]$$

For negative-γ nuclei, this has the form

$$\bar{S}(\omega) \sim \exp\{i\phi^{\text{tot}}\} L(\omega; \Delta\omega_0^j, \lambda), \qquad [90]$$

for the simple one-pulse case. $\bar{S}(\omega)$ has the same form for negative-γ spectral as the ordinary spectral function $S(\omega)$ has for positive-γ signals (Eq. [82]). If $\bar{S}$ is used, the spectral peaks are no longer quadrature images and appear at the true rotating-frame frequency coordinates $\Delta\omega_0^j$.

To conform to the convention for presenting chemical shifts, the spectral function $\bar{S}(\omega)$ must now be plotted ''from right to left,'' i.e., with negative frequency coordinates $\omega < 0$ on the right, positive frequency coordinates $\omega > 0$ on the left, and zero frequency $\omega = 0$ at the center. The labeling of the frequency axis should also conform to this reversal. This is illustrated in Fig. 5.

There is a different scheme to rationalize the spectral presentation for negative-γ nuclei, which avoids the right-to-left plotting of the spectral function $\bar{S}(\omega)$. To avoid further confusion, this discussion is relegated to an Appendix.

EXAMPLES

The points made above are now illustrated by two very simple examples. The first example illustrates the necessity of labeling the spectral frequency axis consistently, in order to assign the spectral peaks to particular spin coherences. This is important when spectral features are used as a diagnostic of particular operator components of the spin-density operator. The second example shows that correct frequency axis labeling must be accompanied by a careful treatment of the sign of phase shifts during excitation pulse sequences.

These two examples are chosen for their simplicity and unambiguity. The issues raised are ubiquitous and further cases abound.

Example 1. Heteronuclear Two-Spin Order

A heteronuclear system of two spins-$\frac{1}{2}$ I and S has four high-field energy eigenstates, denoted $|\alpha\alpha\rangle$, $|\beta\alpha\rangle$, $|\alpha\beta\rangle$, and $|\beta\beta\rangle$, with the notation $|m_{\text{I}}, m_{\text{S}}\rangle$, where m_{I} is the angular momentum of the I spins along the field, and m_{S} is the angular momentum of the S spins along the field. The weakly coupled laboratory-frame spin Hamiltonian, in the absence of RF fields, is

$$H_0^L = \omega_0^{\text{I}} I_z + \omega_0^{\text{S}} S_z + 2\pi J I_z S_z, \qquad [91]$$

with the Larmor frequencies

$$\omega_0^{\text{I}} = -\gamma_{\text{I}} B_0$$
$$\omega_0^{\text{S}} = -\gamma_{\text{S}} B_0, \qquad [92]$$

ignoring chemical shifts. The magnetogyric ratios of the two species are γ_{I} and γ_{S}. In the discussion below, it is assumed that the S spins are observed.

For a heteronuclear spin system, the appropriate ''doubly rotating-frame'' transformation is given by Eq. [28], with the transformation operator

$$V(t) = \exp\{-i[(\omega_{\text{frame}}^{\text{I}} t + \phi_{\text{frame}}^{\text{I}}) I_z + (\omega_{\text{frame}}^{\text{S}} t + \phi_{\text{frame}}^{\text{S}}) S_z]\}. \qquad [93]$$

The rotating-frame frequencies $\omega_{\text{frame}}^{\text{I}}$ and $\omega_{\text{frame}}^{\text{S}}$ for the two channels are equal in magnitude to the RF carrier frequencies generated by the synthesizers $|\omega_{\text{carrier}}^{\text{I}}|$ and $|\omega_{\text{carrier}}^{\text{S}}|$, but with a sign change in the case of positive magnetogyric ratio:

$$\omega_{\text{frame}}^{\text{I}} = -(\text{sign } \gamma_{\text{I}})|\omega_{\text{carrier}}^{\text{I}}|$$
$$\omega_{\text{frame}}^{\text{S}} = -(\text{sign } \gamma_{\text{S}})|\omega_{\text{carrier}}^{\text{S}}|. \qquad [94]$$

The sense of rotation of the frame for a particular spin species is equal to the sense of the spin precession. The initial phases of the rotating frames for the two species, $\phi_{\text{frame}}^{\text{I}}$ and $\phi_{\text{frame}}^{\text{S}}$, are conventionally chosen according to the signs of the magnetogyric ratios, as in Eq. [35].

The doubly rotating-frame free-precession Hamiltonian is

$$H_0 = \Delta\omega_0^{\text{I}} I_z + \Delta\omega_0^{\text{S}} S_z + 2\pi J I_z S_z, \qquad [95]$$

with the resonance offsets

$$\Delta\omega_0^{\text{I}} = \omega_0^{\text{I}} - \omega_{\text{frame}}^{\text{I}}$$
$$\Delta\omega_0^{\text{S}} = \omega_0^{\text{S}} - \omega_{\text{frame}}^{\text{S}}. \qquad [96]$$

In the absence of RF irradiation, the S-spin spectrum consists of two peaks. Each peak is associated with a (-1)-quantum coherence between one of the two pairs of energy eigenstates $\{|\alpha\alpha\rangle, |\alpha\beta\rangle\}$ and $\{|\beta\alpha\rangle, |\beta\beta\rangle\}$. The quadrature S-spin signal is given by

$$s_{\text{S}}(t) \sim 2i\rho_{\boxed{\alpha-}}(t) + 2i\rho_{\boxed{\beta-}}(t), \qquad [97]$$

with the following notation for the rotating-frame coherences (*26*):

$$\rho_{\boxed{\alpha-}} = \langle\alpha\beta|\rho|\alpha\alpha\rangle$$
$$\rho_{\boxed{\beta-}} = \langle\beta\beta|\rho|\beta\alpha\rangle. \qquad [98]$$

Here ρ is the rotating-frame spin-density operator (Eq. [45]). Loosely speaking, $\rho_{\boxed{\alpha-}}(t)$ is called the (-1)-quantum coherence of spins S with spins I in the $|\alpha\rangle$ state, while $\rho_{\boxed{\beta-}}$ is called the (-1)-quantum coherence of spins S with spins I in the $|\beta\rangle$ state.

The two coherences evolve according to the equation

$$\rho_{\alpha-}(t) = \rho_{\boxed{\alpha-}}(0)\exp\{(i\omega_{\boxed{\alpha-}} - \lambda)t\}$$
$$\rho_{\beta-}(t) = \rho_{\boxed{\beta-}}(0)\exp\{(i\omega_{\boxed{\beta-}} - \lambda)t\}, \qquad [99]$$

where $\lambda = T_2^{-1}$ is the coherence dephasing rate constant (assumed, for simplicity, to be the same for the two coherences). The rotating-frame precession frequencies are

$$\omega_{\boxed{\alpha-}} = \langle\alpha\alpha|H_0|\alpha\alpha\rangle - \langle\alpha\beta|H_0|\alpha\beta\rangle = \Delta\omega_0^S + \pi J$$
$$\omega_{\boxed{\beta-}} = \langle\beta\alpha|H_0|\beta\alpha\rangle - \langle\beta\beta|H_0|\beta\beta\rangle = \Delta\omega_0^S - \pi J. \quad [100]$$

The S-spin spectrum is given in general by a sum of two Lorentzians

$$S_S(\omega) \sim a_{\boxed{\alpha-}} L(\omega; \omega_{\boxed{\alpha-}}, \lambda) + a_{\boxed{\beta-}} L(\omega; \omega_{\boxed{\beta-}}, \lambda), \quad [101]$$

with the complex peak amplitudes

$$a_{\boxed{\alpha-}} = 2i\rho_{\boxed{\alpha-}}(0)$$
$$a_{\boxed{\beta-}} = 2i\rho_{\boxed{\beta-}}(0). \qquad [102]$$

According to Eq. [100], the $\rho_{\boxed{\alpha-}}$ peak appears on the positive frequency side of the $\rho_{\boxed{\beta-}}$ peak, in the case of positive J. This positions the $\rho_{\boxed{\alpha-}}$ peak on the right-hand side of the $\rho_{\boxed{\beta-}}$ peak if γ_S is positive (Fig. 6a). The peaks are the other way round if the J coupling is negative (Fig. 6c).

Both peaks have real positive amplitudes if the S-spin signal is induced by a strong $\pi/2$ pulse of phase 0, applied

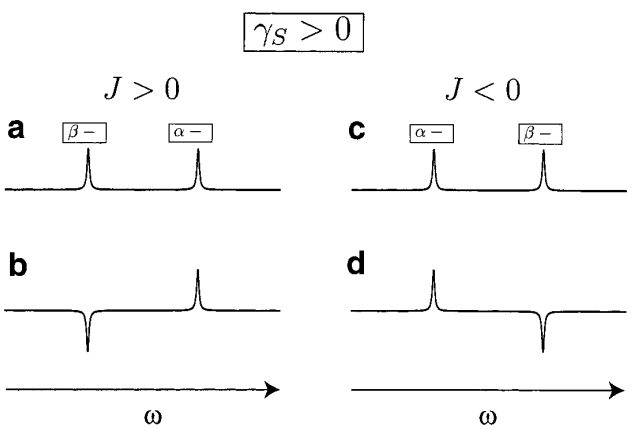

FIG. 6. Spin-state assignments of the S-spin spectral peaks in a heteronuclear two-spin-$\frac{1}{2}$ system, for the case of positive magnetogyric ratio γ_S. (Left) Spin–spin coupling constant $J > 0$. (Right) Spin–spin coupling constant $J < 0$. (a, c) Spectral appearance and peak assignments for an initial rotating-frame density operator $\rho(0) \sim -S_y$. (b, d) Spectral appearance and peak assignments for an initial rotating-frame density operator $\rho(0) \sim -2I_zS_y$.

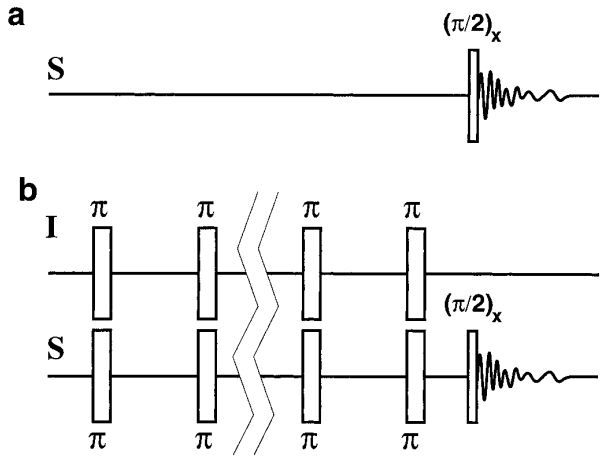

FIG. 7. Illustrative pulse sequences. (a) Simple one-pulse sequence to generate in-phase S-spin signal. (b) Generation of two-spin Zeeman order through cross-correlated relaxation. The $\pi/2$ pulse on the S spins is preceded by a long repeating sequence of simultaneous π pulses at the I-spin and the S-spin Larmor frequencies. The interval between the π pulses is short compared to T_1. The entire synchronous π pulse sequence is long compared to T_1.

to a spin ensemble in equilibrium (Fig. 7a). This is easily seen by expanding the density operator after the pulse in terms of the shift and polarization operators:

$$\rho(0) \sim \exp\left\{-i\frac{\pi}{2}S_x\right\}S_z\exp\left\{i\frac{\pi}{2}S_x\right\}$$
$$= -S_y$$
$$= -\frac{1}{2i}(I^\alpha + I^\beta)(S^+ - S^-)$$
$$= \frac{1}{2i}I^\alpha S^- + \frac{1}{2i}I^\beta S^- - \frac{1}{2i}I^\alpha S^+ - \frac{1}{2i}I^\beta S^+. \quad [103]$$

The coherence amplitudes at the start of signal acquisition are therefore

$$\rho_{\boxed{\alpha-}}(0) = \rho_{\boxed{\beta-}}(0) = \frac{1}{2i}, \qquad [104]$$

leading to the spectral peak amplitudes

$$a_{\boxed{\alpha-}} = 2i\rho_{\boxed{\alpha-}}(0) = 1$$
$$a_{\boxed{\beta-}} = 2i\rho_{\boxed{\beta-}}(0) = 1. \qquad [105]$$

The two Lorentzian peaks are in absorption and have equal amplitude.

Now consider the experiment shown in Fig. 7b, which has been used to probe cross-correlated relaxation effects (*8, 9*). A long repeating sequence of synchronous π pulses is applied

to both spin species, for a total time long compared to the spin–lattice relaxation time constants. If the relaxation is caused by random reorientation of the dipole–dipole coupling as well as the S-spin chemical-shift anisotropy tensor, and if these two stochastic processes display a significant cross correlation, then a state of significant two-spin Zeeman order gradually builds up under the synchronous π pulse train. The density operator at the end of the π pulse train is therefore

$$\rho \sim \kappa 2I_zS_z, \qquad [106]$$

where κ is a real number depending on the cross correlation. The density operator at the beginning of signal acquisition is

$$\begin{aligned}\rho(0) &\sim \kappa \exp\left\{-i\frac{\pi}{2}S_x\right\}2I_zS_z\exp\left\{i\frac{\pi}{2}S_x\right\}\\ &= -\kappa 2I_zS_y\\ &= -\frac{\kappa}{2i}(I^\alpha - I^\beta)(S^+ - S^-)\\ &= \frac{\kappa}{2i}I^\alpha S^- - \frac{\kappa}{2i}I^\beta S^- + \frac{\kappa}{2i}I^\alpha S^+ - \frac{\kappa}{2i}I^\beta S^+, \qquad [107]\end{aligned}$$

corresponding to the following initial amplitudes of the observable S-spin coherences:

$$\begin{aligned}\rho_{\boxed{\alpha-}}(0) &= \frac{\kappa}{2i}\\ \rho_{\boxed{\beta-}}(0) &= -\frac{\kappa}{2i}. \qquad [108]\end{aligned}$$

The spectral peak amplitudes are

$$\begin{aligned}a_{\boxed{\alpha-}} &= 2i\rho_{\boxed{\alpha-}}(0) = \kappa\\ a_{\boxed{\beta-}} &= 2i\rho_{\boxed{\beta-}}(0) = -\kappa. \qquad [109]\end{aligned}$$

This time, the two Lorentzian peaks have opposite signs. This ''antiphase'' spectral pattern is a signature of two-spin Zeeman order before the final $\pi/2$ pulse.

Observe the following points:

1. The sign of κ is related to the sign of the cross-correlated relaxation mechanisms active during the synchronous π pulse sequence. It is vital for the interpretation of the experiment that the sign of κ is deduced correctly from the experimental spectrum.

2. The sign of κ can be deduced correctly only if the spectral peaks are associated with the correct pairs of spin states. A positive value of κ is associated with an antiphase pattern in which the $\rho_{\boxed{\beta-}}$ peak is inverted in amplitude, while the $\rho_{\boxed{\alpha-}}$ peak is noninverted.

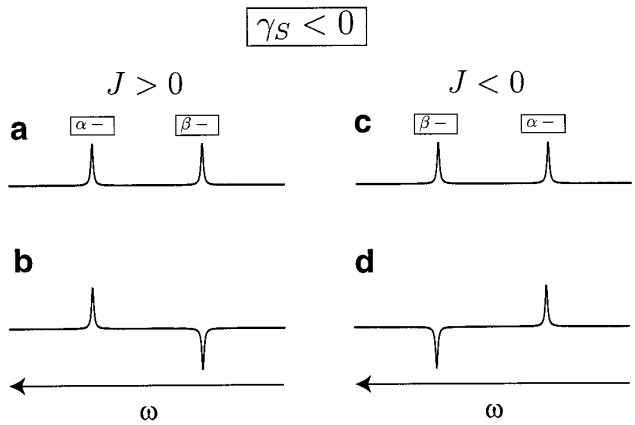

FIG. 8. Spin-state assignments of the S-spin spectral peaks in a heteronuclear two-spin-$\frac{1}{2}$ system, for the case of negative magnetogyric ratio γ_S. (Left) Spin–spin coupling constant $J > 0$. (Right) Spin–spin coupling constant $J < 0$. (a, c) Spectral appearance and peak assignments for an initial rotating-frame density operator $\rho(0) \sim -S_y$. (b, d) Spectral appearance and peak assignments for an initial rotating-frame density operator $\rho(0) \sim -2I_zS_y$.

3. The assignment of spectral peaks to particular coherences depends on knowledge of the sign of the J coupling, and an algebraically consistent labeling of the spectral frequency axis. For positive J, the $\rho_{\boxed{\alpha-}}$ peak has a higher frequency than the $\rho_{\boxed{\beta-}}$ peak. Hence, for positive γ_S, the $\rho_{\boxed{\alpha-}}$ peak appears to the right of the $\rho_{\boxed{\beta-}}$ peak in the spectrum. In this case, positive two-spin Zeeman order appears as a ''down–up'' spectral pattern, reading the spectrum from left to right.

The peak assignments and correctly labeled frequency axes for various sign combinations of J and γ_S are shown in Fig. 6 and Fig. 8.

The interpretation of antiphase spectral patterns is very intuitive if a rationalized frequency axis is used. The peak with the ''α'' label is shifted along the frequency axis in the same sense as the spin–spin coupling J. The assignment of peaks to spin states is much less obvious using the frequency axis labeling scheme in common use today, which takes no account of the sign of the Larmor frequency.

This example is particularly clear because the creation of two-spin order does not require any phase-shifted pulses. Pulse sequences which rely on the J couplings to induce two-spin Zeeman order, for example, INEPT (*27*), raise separate issues as to the sign of the radiofrequency phase shifts, to be discussed in the next section.

Example 2. A Two-Pulse Sequence

Consider a sample containing two sets of sites, j and k, each occupied by spins-$\frac{1}{2}$. The magnetogyric ratio γ of the spins is assumed to be positive, and sites j are more shielded than sites k. The carrier frequency is chosen such that the

rotating-frame frequency is the exact mean of the two precession frequencies. The resonance offsets of the spins, with respect to the rotating-frame frequency, are

$$\Delta\omega_0^j = \tfrac{1}{2}\omega_\Delta$$
$$\Delta\omega_0^k = -\tfrac{1}{2}\omega_\Delta, \qquad [110]$$

where ω_Δ is the shift difference in frequency units,

$$\omega_\Delta = -\omega_0(\sigma^j - \sigma^k), \qquad [111]$$

positive by definition since ω_0 is negative. If spin–spin couplings are negligible, the spectrum consists of two peaks with the peak associated with spins in sites j to the right of that associated with spins in sites k (Fig. 9a). Transverse magnetization associated with spins in sites j precesses in the positive (anticlockwise) direction in the rotating frame. Transverse magnetization associated with spins in sites k precesses in the negative (clockwise) direction in the rotating frame.

Now examine the dynamics of the spins under the very simple radiofrequency pulse sequence in Fig. 10. This consists of two $\pi/2$ pulses separated by a delay $\tau = |\pi/\omega_\Delta|$ with the second pulse shifted in phase by $\pi/2$. During the precession interval, the transverse magnetization components of the two sites precess through an angle $\pi/2$, in opposite directions.

The term ''phase of the pulse'' is taken here to refer to the phase of the rotating-frame nutation axis during the pulse,

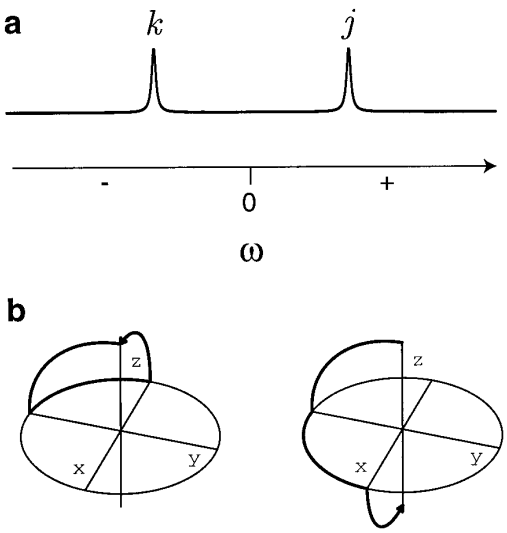

FIG. 9. Spectrum and spin dynamics of a system with two independent spin-$\frac{1}{2}$ sites, j and k, where j is more shielded than k and the spins have positive magnetogyric ratio. (a) Schematic spectrum. (b) (Left) Magnetization trajectory of spins k; (Right) magnetization trajectory of spins j during the two-pulse sequence in Fig. 10.

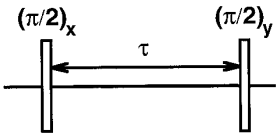

FIG. 10. Simple two-pulse sequence for illustrating the sign behavior of radiofrequency phase shifts. The subscripts x and y refer to the nutation axis phases $\phi_p = 0$ and $\pi/2$, but are usually misinterpreted as referring to the electronic carrier wave phase ψ_p during the pulse. ϕ_p and ψ_p have opposite signs for spins of positive γ.

notated ϕ_p in the above discussion. A pulse $(\pi/2)_x$ rotates the spin magnetization through an angle $\pi/2$ about the rotating-frame x axis, while a pulse $(\pi/2)_y$ rotates the spin magnetization through an angle $\pi/2$ about the rotating-frame y axis.

Suppose the pulse sequence is applied to thermal equilibrium z magnetization. Calculation of the result is elementary and is visualized in Fig. 9b. The z magnetization of spins in the more shielded sites j is inverted, while the z magnetization of spins in the less-shielded sites k is returned to equilibrium.

This is clearly a completely different physical situation from one in which the magnetization of the k spins is inverted, while that of the j spins is returned to equilibrium. The physical distinction may be very sharp if, for example, the spins in sites j and sites k have different spin–lattice relaxation characteristics.

Note that the result shown in Fig. 9 is *not* obtained if this simple sequence is programmed naively on current instruments. It is easily verified that naive programming of the radiofrequency carrier phase ψ_p inverts the magnetization of the *less*-shielded sites, while returning the magnetization of the *more*-shielded sites to equilibrium. The fate of the magnetizations is easily determined by applying a further $\pi/2$ pulse to convert the longitudinal magnetization into observable coherences. Phase cycling may be used if necessary to remove signal components from transverse magnetization left over by the two-pulse sequence.

This discrepancy is due to the fact that the rotating-frame nutation axes are shifted in phase by ϕ_p, which is opposite in sign to the carrier phase ψ_p for positive-γ spins. This elementary discrepancy may have gone unnoticed because of the simultaneous confusion around the labeling of the frequency axis. The usual frequency axis, increasing from right to left, has often been misinterpreted as the precession frequency in the rotating frame. This leads to one sign error, which cancels the error in the sign of the nutation axis phases. The previous example showed, however, that it is desirable to label the frequency axis carefully, in order to be consistent with the sign of the spin interactions. Correction of one error makes the second error obvious. The sign discrepancies cannot be fixed one at a time. A global rationalization of sign usage is unavoidable.

IMPLICATIONS AND RECOMMENDATIONS

This article should have made it obvious that the subject of signs in NMR is very confusing and delicate. Fortunately, the conclusions of this article may be distilled into a few rather simple software recommendations.

Recommendation 1. A Software Flag for the Sign of the Magnetogyric Ratio

The software should require that the spectrometer operator sets a flag for the sign of γ for the spins under observation. This flag is then consulted by the pulse programming software and the data processing code.

Recommendation 2. Radiofrequency Phases Should Take into Account the Sign of γ

The spectrometer operator desires control over the phases ϕ_p of the rotating-frame nutation axes. The absolute electronic phase ψ_p during the pulse is not of direct interest. It would be most convenient if pulse programs referred to the nutation axis phases ϕ_p. The software translates these instructions into code for the electronics, taking into account the sign of γ. For positive γ, the pulse programmer software implements RF synthesizer phase shifts ψ_p which are minus the values in the pulse program. If γ is negative, there is no sign change.

The radiofrequency receiver reference phase ϕ_{rec} is handled in similar fashion. The user specifies the value of ϕ_{rec} in pulse programs. The software converts this into a phase shift ψ_{rec} of the carrier wave during detection, taking into account the sign of γ. For positive γ, there is a sign change. For negative γ, there is no sign change.

Recommendation 3. The Post-digitization Phase Shift Should Take into Account the Sign of γ

The post-digitization phase shift implemented by ''data-swapping'' routines at the output of the ADCs should experience identical treatment. The ''γ-sensitive post-digitization phase shift'' $\phi_{\mathrm{post\,dig}}$ appears in the pulse program text. The software interprets this as an absolute phase shift $\psi_{\mathrm{post\,dig}} = -\phi_{\mathrm{post\,dig}}$ if γ is positive, but as $\psi_{\mathrm{post\,dig}} = +\phi_{\mathrm{post\,dig}}$ if γ is negative. In each case, the digitized quadrature signal is multiplied by the factor $\exp\{i\psi_{\mathrm{post\,dig}}\}$ before transfer to the signal accumulation device. Post-digitization phase shifts in multiples of $\pi/2$ may be implemented in the hardware by a channel-swapping/sign-inversion scheme, such as that given in Eq. [57] for the case $\psi_{\mathrm{post\,dig}} = \pi/2$.

The post-digitization phase shift $\phi_{\mathrm{post\,dig}}$ and the receiver phase shift ϕ_{rec} should be clearly differentiated. They are only equivalent if the receiver is perfectly adjusted.

Recommendation 4. Spectral Frequency Axes Should Represent True Rotating-Frame Precession Frequencies

For *positive γ nuclei*, the spectral function $S(\omega)$ should be derived by standard Fourier transformation of the digitized signal $s(t)$. The spectral function $S(\omega)$ should be plotted according to the usual mathematical convention, with negative frequencies on the left, and positive frequencies on the right. Less-shielded spins appear on the left of the spectrum, well-shielded spins appear on the right. The ''deshielding'' ppm scale increases from right to left.

When a spectral frequency scale is used, it should employ the correct values of ω: negative on the left, and positive on the right. A peak at the center of the spectrum $\omega = 0$ corresponds to spins whose precession frequency has the same magnitude as the spectrometer carrier frequency, but opposite in sign: $\omega_0^j = -|\omega^{\mathrm{carrier}}|$. The spectral frequency coordinate of each peak corresponds to the rotating-frame precession frequency of the corresponding magnetization component. If these recommendations are followed, spin dynamical calculations may use the nutation axis phases which appear in the pulse program, and the rotating-frame frequencies which appear along the frequency axis.

For *negative γ nuclei*, the spectral function $\bar{S}(\omega)$ should be derived by Fourier transforming the complex conjugate of the digitized signal $s(t)^*$. The spectral function $\bar{S}(\omega)$ is plotted backward, with frequency increasing from right to left. This ensures that less-shielded spins again appear on the left of the spectrum, while well-shielded spins appear on the right. The deshielding ppm scale increases as usual from right to left.

For negative γ, the spectral frequency scale should indicate positive frequencies on the left, and negative frequencies on the right. A peak at the center of the spectrum $\omega = 0$ corresponds to spins whose precession frequency is the same as the spectrometer carrier frequency: $\omega_0^j = |\omega^{\mathrm{carrier}}|$. Spin dynamical calculations may be based on the nutation axis phases which appear in the pulse program, and the rotating-frame precession frequencies which appear along the frequency axis.

If these recommendations are implemented, the plotted spectra contain peaks at the frequencies of the observable (-1)-quantum coherences, independent of the sign of γ. Phase cycles may be calculated on the basis that all coherence-transfer pathways terminate with coherence order $= -1$. Phase cycles written in terms of the nutation axis phases ϕ_p, receiver phase ϕ_{rec}, and post-digitization phase shift $\phi_{\mathrm{post\,dig}}$ are the same for nuclei of positive and negative γ.

These recommendations may appear quite complex. However, by and large, *they are not conventions.* There are only three occasions in which true conventions intrude, and none are controversial: (i) the convention that the rotating-frame z axis is along the magnetic field direction; (ii) the convention of using a right-handed axis system; (iii) the convention

that the spectrum is plotted with the shielding scale increasing from left to right. The remaining consequences follow from the physical properties of the spins themselves and the actual hardware settings of normal quadrature receivers. I believe that the above recommendations are a viable long-term option, allowing spectroscopists to label NMR spectra, calculate spin dynamics, and interpret signed interactions in a confident and self-evident fashion.

APPENDIX

Alternative Processing Scheme for Negative-γ Nuclei

In the above discussion, it was concluded that the correct data processing for negative-γ nuclei is to take the complex conjugate of the time-domain signal $s(t)$ before Fourier transformation, followed by plotting of the resulting function $\bar{S}(\omega)$ with the frequency coordinate ω increasing from right to left. As discussed above, the peaks in the spectrum are then associated with rotating-frame (-1)-quantum coherences, and their frequency coordinates correspond directly to the rotation frequencies of the transverse magnetization components in the rotating frame.

This is conceptually rather clear cut, but the extent of software reprogramming is perhaps undesirable. An equivalent effect is achieved by a simple subterfuge. Suppose that the time-domain signal is left unchanged, an ordinary Fourier transform is applied, and the spectrum plotted in the usual mathematical sense with the frequency coordinate increasing from left to right. If the complex conjugate of *the spectrum* is taken, and the sense of the *axis labeling* (but only the labeling!) is reversed, then the result is almost identical to the ''correct'' procedure indicated above. This may be seen from the identity

$$S(\omega) = \bar{S}(-\omega)^*, \qquad [112]$$

where $S(\omega)$ is the result of Fourier transforming $s(t)$, while $\bar{S}(\omega)$ is the result of Fourier transforming $s(t)^*$:

$$S(\omega) = \int_0^\infty s(t)\exp\{-i\omega t\}\,dt$$

$$\bar{S}(\omega) = \int_0^\infty s(t)^*\exp\{-i\omega t\}\,dt. \qquad [113]$$

Now since the ''reversed'' frequency axis labeling is done anyway on current instruments, it turns out that this procedure is by chance almost exactly equal to that performed already! The only discrepancy is that the complex conjugate of the spectrum should be taken, i.e., the imaginary component of the spectrum should be reversed in sign. The ''correct'' presentation of the spectrum for negative-γ spins, as shown in Fig. 5, is fortuitously already achieved on current instruments, with the minor difference that the imaginary part of the spectrum has the wrong sign.

Nevertheless, I feel that the ''rigorous'' procedure described in the main text is preferable.

ACKNOWLEDGMENTS

This research has been supported by the Swedish Natural Science Research Foundation. I thank Lorenzo di Bari, Mattias Edén, and Torgny Karlsson for performing experiments in which these issues surfaced with particular clarity. I also thank Professor R. R. Ernst and Professor B. Gerstein for critical comments, and C. Bronniman for discussions.

REFERENCES

1. D. P. Raleigh, M. H. Levitt, and R. G. Griffin, *Chem. Phys. Lett.* **146,** 71 (1988).
2. M. G. Colombo, B. H. Meier, and R. R. Ernst, *Chem. Phys. Lett.* **146,** 189 (1988).
3. M. H. Levitt, D. P. Raleigh, F. Creuzet, and R. G. Griffin, *J. Chem. Phys.* **92,** 6347 (1990).
4. L. G. Werbelow and D. M. Grant, *Adv. Magn. Reson.* **9,** 189 (1977).
5. M. Goldman, *J. Magn. Reson.* **60,** 437 (1984).
6. C. Dalvit and G. Bodenhausen, *Chem. Phys. Lett.* **161,** 554 (1989).
7. L. Di Bari, J. Kowalewski, and G. Bodenhausen, *J. Chem. Phys.* **93,** 7698 (1990).
8. M. H. Levitt and L. Di Bari, *Phys. Rev. Lett.* **69,** 3124 (1992).
9. M. H. Levitt and L. Di Bari, *Bull. Magn. Reson.* **16,** 92 (1994).
10. R. Bowtell, R. M. Bowley, and P. Glover, *J. Magn. Reson.* **88,** 643 (1990).
11. H. T. Edzes, *J. Magn. Reson.* **86,** 293 (1990).
12. W. S. Warren, W. Richter, A. H. Andreotti, and B. T. Farmer, *Science* **262,** 2005 (1993).
13. M. H. Levitt, *Concepts Magn. Reson.* **8,** 77 (1996).
14. M. Goldman, V. Fleury, and M. Guéron, *J. Magn. Reson. A* **118,** 11 (1996).
15. T. G. Oas, R. G. Griffin, and M. H. Levitt, *J. Chem. Phys.* **89,** 692 (1988).
16. M. H. Levitt, T. G. Oas, and R. G. Griffin, *Isr. J. Chem.* **28,** 271 (1988).
17. C. Bronnimann, private communication.
18. O. N. Antzutkin, S. C. Shekar, and M. H. Levitt, *J. Magn. Reson. A* **115,** 7 (1995).
19. M. Mehring and J. S. Waugh, *Rev. Sci. Instrum.* **43,** 649 (1972).
20. M. M. Maricq, *Phys. Rev. B* **25,** 6622 (1982).
21. A. Abragam, ''The Principles of Nuclear Magnetism,'' Clarendon Press, Oxford, 1961.
22. R. R. Ernst, G. Bodenhausen, and A. Wokaun, ''Principles of Nuclear Magnetic Resonance in One and Two Dimensions,''p. 120. Clarendon Press, Oxford, 1987, p. 120.
23. G. Bodenhausen, H. Kogler, and R. R. Ernst, *J. Magn. Reson.* **58,** 370 (1984).
24. D. I. Hoult and R. E. Richards, *Proc. R. Soc. London Ser. A* **344,** 311 (1975).
25. R. N. Bracewell, ''The Fourier Transform and Its Applications,'' McGraw–Hill, New York, 1986.
26. M. H. Levitt, C. Radloff, and R. R. Ernst, *Chem. Phys. Lett.* **114,** 435 (1985).
27. G. A. Morris and R. Freeman, *J. Am. Chem. Soc.* **101,** 760 (1979).